Supplementary Material Available

Complete lists of intramolecular (Table I) and intermolecular (Table II) hydrogen bond lengths and angles, as well as results of solvent accessibility calculations for amide hydrogens (Table III) (6 pages). Ordering information is given on any current masthead page.

Registry No. RNase A, 9001-99-4.

References

Borkakoti, N., Moss, D. A., & Palmer, R. A. (1982) *Acta Crystallogr., Sect. B B38*, 2210-2217.

Hamilton, W. C., Rollett, J. S., & Sparks, R. A. (1965) *Acta Crystallogr. 18*, 129-130.

Hanson, J., & Schoenborn, B. P. (1981) *J. Mol. Biol. 153*, 117-146.

Hendrickson, W. A., & Konnert, J. H. (1981) in *Biomolecular Structure, Conformation, Function, and Evolution* (Srinivasan, R., Ed.) Vol. 1, pp 43-57, Pergamon Press, Oxford.

Jones, T. A. (1978) *J. Appl. Crystallogr. 11*, 268-272.

Kossiakoff, A. A. (1982) *Nature (London) 296*, 713-721.

Kossiakoff, A. A., & Spencer, S. A. (1980) *Nature (London) 288*, 414-416.

Kossiakoff, A. A., & Spencer, S. A. (1981) *Biochemistry 20*, 6462-6474.

Lenhert, P. G. (1975) *J. Appl. Crystallogr. 8*, 568-570.

Luzzati, V. (1952) *Acta Crystallogr. 5*, 802-810.

North, A. C. T., Phillips, D. C., & Mathews, F. S. (1968) *Acta Crystallogr., Sect. A A24*, 351-359.

Phillips, S. E. V., & Schoenborn, B. P. (1981) *Nature (London) 292*, 81-82.

Powers, T. B. (1976) Ph.D. Thesis, Yale University.

Prince, E., Wlodawer, A., & Santoro, A. (1978) *J. Appl. Crystallogr. 11*, 173-178.

Rosa, J. J., & Richards, F. M. (1981) *J. Mol. Biol. 145*, 835-851.

Santoro, A., & Wlodawer, A. (1980) *Acta Crystallogr., Sect. A A36*, 442-450.

Schreier, A. A., & Baldwin, R. L. (1976) *J. Mol. Biol. 105*, 409-426.

Sjölin, L., & Wlodawer, A. (1981) *Acta Crystallogr., Sect. A A37*, 594-604.

Wlodawer, A. (1980) *Acta Crystallogr., Sect. B B36*, 1826-1831.

Wlodawer, A., & Sjölin, L. (1981) *Proc. Natl. Acad. Sci. U.S.A. 78*, 2853-2855.

Wlodawer, A., & Hendrickson, W. A. (1982) *Acta Crystallogr., Sect. A A38*, 239-247.

Wlodawer, A., & Sjölin, L. (1982) *Proc. Natl. Acad. Sci. U.S.A. 79*, 1418-1422.

Wlodawer, A., Bott, R., & Sjölin, L (1982) *J. Biol. Chem. 257*, 1325-1332.

Wyckoff, H. W., Tsernoglou, D., Hanson, A. W., Knox, J. R., Lee, B., & Richards, F. M. (1970) *J. Biol. Chem. 245*, 305-328.

Plasma Actin Depolymerizing Factor Has both Calcium-Dependent and Calcium-Independent Effects on Actin†

Harriet E. Harris and Alan G. Weeds*

ABSTRACT: The effects of pig plasma actin depolymerizing factor (ADF) on both G-actin polymerization and F-actin fragmentation have been examined by using rabbit skeletal muscle actin labeled with *N*-(1-pyrenyl)iodoacetamide, a sensitive fluorescent probe for monomer to filament interconversion. Fluorescence data have been compared with results obtained by viscometry and by difference absorption measurements at 232 nm. Plasma ADF nucleates actin filament assembly in a Ca^{2+}-dependent manner; actin polymerization rates are enhanced at greater than 10^{-6} M Ca^{2+}. The calcium concentration dependence of this effect, showing a shift in ADF nucleating capacity between 10^{-6} and 10^{-7} M Ca^{2+}, is that expected for an intracellular regulatory effect, but in plasma, the protein would always be saturated with Ca^{2+}. Although the rate of polymerization is markedly enhanced in the presence of calcium ions, the extent of polymerization (as determined by the amplitude of the fluorescence change or the specific viscosity) is reduced in the presence of ADF and shows little or no Ca^{2+} dependence. The critical concentration of actin monomers is increased in the presence of ADF whether calcium is present or not. When ADF is added to F-actin, there is an immediate fall in fluorescence. This conversion of filaments to monomers by ADF (as defined by the fluorescence changes) is unaffected by calcium concentration. Electron micrographs of F-actin treated with ADF show that the filaments are indeed shortened at both high and low calcium concentrations. Taken together, these observations are interpreted in terms of a model in which ADF has both Ca^{2+}-sensitive and Ca^{2+}-insensitive binding sites for actin.

Plasma actin depolymerizing factor (ADF)[1] is a protein which disrupts actin filaments and is found in relatively large amounts in plasma and serum from a variety of species (Norberg et al., 1979; Chaponnier et al., 1979; Harris et al., 1980; Harris & Schwartz, 1981). Filament fragmentation has been observed by electron microscopy and monitored by viscosity and sedimentation studies. In addition, the DNase inhibition assay has shown that ADF acts rapidly on actin

† From the MRC Laboratory of Molecular Biology, University Medical School, Cambridge CB2 2QH, U.K. *Received August 3, 1982.*

[1] Abbreviations: ADF, plasma actin depolymerizing factor; PMSF, phenylmethanesulfonyl fluoride; DTT, dithiothreitol; EGTA, ethylene glycol bis(β-aminoethyl ether)-*N*,*N*,*N*′,*N*′-tetraacetic acid; $NaDodSO_4$, sodium dodecyl sulfate; Tris, tris(hydroxymethyl)aminomethane; Bicine, *N*,*N*-bis(2-hydroxyethyl)glycine.

0006-2960/83/0422-2728$01.50/0

filaments to release a nonsedimentable form of actin (monomers or complexes of ADF and G-actin) that inhibits DNase activity, and this action is not dependent on calcium concentration (Harris & Gooch, 1981; Harris et al., 1982). Indeed, a protein with a likely function of scavenging actin filaments in plasma, where calcium concentration is always in the millimolar range, is not expected to be regulated by calcium. However, ADF is stabilized against heat denaturation by calcium (Harris et al., 1980) and therefore binds Ca^{2+}.

Recently, it has become apparent that plasma ADF is functionally similar to gelsolin. This protein, originally isolated from alveolar macrophages, solvates actin gels in a Ca^{2+}-dependent manner and is thought to regulate the gel–sol transformation in the cytoplasm (Yin & Stossel, 1979; Yin et al., 1980). In addition to these effects on actin filaments, gelsolin increases the rate of nucleation of actin, producing a larger number of shorter filaments: it binds to the "barbed" ends of these filaments (Yin et al., 1981b), thereby preventing elongation at the preferred assembly end (Pollard & Mooseker, 1981). In both situations, the overall effect is to produce shorter F-actin filaments. A protein of similar molecular weight (M_r) has been isolated from platelets and shown to accelerate G-actin polymerization; it also binds to the barbed ends of filaments (Wang & Bryan, 1981).

It now appears that gelsolin and plasma ADF are structurally related. Both have molecular weights of 91 000–92 000 and isoelectric points of 6.1 and about 6–6.5, respectively (Yin & Stossel, 1980; Harris & Gooch, 1981). Antiserum to macrophage gelsolin cross-reacts with a M_r 91 000 polypeptide in human plasma and serum (Yin et al., 1981a). Furthermore, pig plasma ADF and gelsolin from pig platelets yield almost identical peptide maps (B. J. Pope, H. E. Harris, and A. G. Weeds, unpublished experiments).

In order to reconcile the discrepant observations that ADF is Ca^{2+} independent and gelsolin Ca^{2+} sensitive, we have reexamined the Ca^{2+} dependence of the effects of ADF on the polymerization of G-actin and on actin filament disassembly. As a probe, we have used actin labeled with *N*-(1-pyrenyl)-iodoacetamide, a fluorescent compound with a spectrum that is a very sensitive indicator of the monomer to filament transition (Kouyama & Mihashi, 1981). Results of these experiments and others using viscometry or electron microscopy show that ADF exhibits both Ca^{2+}-dependent and Ca^{2+}-independent interactions with actin.

Materials and Methods

Pig plasma actin depolymerizing factor was prepared from pig plasma (Harris & Weeds, 1978) which had been stored at −20 °C. Two methods were used for the initial stages of purification. In the early preparations, this involved ammonium sulfate precipitation and DEAE-cellulose chromatography as follows: About 500 mL of frozen plasma was thawed and PMSF added to 1 mM. The plasma was fractionated by addition of solid ammonium sulfate at 4 °C. The fraction precipitating at 40–60% saturation was redissolved in about 100 mL of 20 mM imidazole hydrochloride, pH 6.3, 30 mM NaCl, 10^{-4} M $CaCl_2$, and 1 mM azide and dialyzed to remove residual ammonium sulfate. Protein was applied to a 12 × 10 cm DEAE-cellulose column (Whatman DE-52 cellulose) equilibrated and eluted in the same buffer. ADF eluted at the leading edge of a large peak of unbound protein. The active fractions were pooled and concentrated by ultrafiltration with an Amicon PM10 membrane. In later preparations, plasma was fractionated by precipitation with poly(ethylene glycol) 6000 [adapted from methods described by Polson et al. (1964)] as follows: 1000 mL of plasma was diluted with water to about 1600 mL and adjusted to pH 4.6 with 1 M acetic acid. Poly(ethylene glycol) was added as a 50% w/v solution to a final concentration of 5% and the precipitate removed by centrifugation. Poly(ethylene glycol) was then added to 15% and the precipitate allowed to settle. After the supernatant solution was decanted, 400 mL of 10 mM succinate buffer, pH 6.0, was added containing 10^{-4} M $CaCl_2$ and 1 mM azide and the solution adjusted to pH 6.0 with 2 N NaOH. Following dialysis against 10 mM succinate, pH 6.0, 50 mM NaCl, 10^{-4} M $CaCl_2$, and 1 mM sodium azide, the solution was applied to a carboxymethylcellulose column (6 × 25 cm) equilibrated in the same buffer. The ADF was eluted with a step to 0.35 M NaCl in the same succinate buffer. About 2% of the total protein and 65% of the ADF activity were recovered from this column. Subsequent purification steps were the same for both procedures. Further fractionation was achieved on a 1.5 × 100 cm column of carboxymethylcellulose (Whatman CM-52 cellulose). Column and sample were both equilibrated in 10 mM succinate, pH 6.0, 50 mM NaCl, 10^{-4} M $CaCl_2$, and 1 mM azide; 1 mM PMSF was included in all column buffers and 1 mM diisopropyl fluorophosphate added to the sample before loading. The column was washed extensively with the same buffer to remove unbound protein and eluted with a linear gradient of 50–250 mM NaCl in 10 mM succinate, pH 6.0, 10^{-4} M $CaCl_2$, and 1 mM azide (total volume 1 L). Fractions with ADF activity eluted between 100 and 125 mM NaCl: these were pooled, concentrated, and applied to a 1.5 × 20 cm column of hydroxyapatite (Bio-Rad, Bio-Gel HTP) equilibrated in 75 mM sodium phosphate, pH 6.2, and 1 mM azide. Protein was eluted with a linear gradient of 75–350 mM sodium phosphate, pH 6.2 (200 mL total volume). ADF eluted as a single peak, identified by $NaDodSO_4$–polyacrylamide gel electrophoresis and by DNase inhibition activity (Harris et al., 1982). In order to minimize proteolysis, which frequently appeared following hydroxyapatite chromatography, we removed trace contaminants of plasminogen by affinity chromatography on lysine–Sepharose (Chibber et al., 1974) before the hydroxyapatite column, and leupeptin was added to the applied sample and the eluting buffers at 1 $\mu g \cdot mL^{-1}$ together with additional diisopropyl fluorophosphate at 1 mM. In some preparations, contaminating immunoglobulin was removed on a small (1–2 mL) column of protein A covalently bound to Sepharose (Harris & Gooch, 1981). The purified ADF was stored at <4 °C in succinate buffers at pH 6.0, at which pH it is stabilized against proteolysis, and was used within 2 weeks of preparation. Even with these further additions of proteolytic inhibitors, we were unable to eliminate proteolysis completely. Most ADF samples were less than 75% pure, as measured either by gel electrophoresis or by DNase inhibition assay, and the ADF concentration was therefore estimated by assuming a specific activity for pure ADF of 280 units$\cdot mg^{-1}$ (Harris & Gooch, 1981). All columns were run at <4 °C. Human actin depolymerizing factor was prepared by similar methods from human plasma.

ADF Binding to Sepharose–DNase I–Actin Complexes. DNase I covalently linked to Sepharose was prepared and saturated with G-actin as described previously (Harris & Gooch, 1981), giving about 100 μg of actin per mL of slurry. For saturation of this with ADF, whole plasma was passed over DEAE-cellulose as described above and the flowthrough applied in excess (10 mL to 1 mL of slurry) to the Sepharose–DNase–actin. After the resin had been extensively washed with 30 mM NaCl and 20 mM imidazole hydrochloride, pH 7.0, gel electrophoresis showed that ADF (identified as a

component of M_r 92 000) was the only polypeptide bound. Conditions for eluting ADF, using EGTA-containing buffers or denaturing agents, were tested by using small (1-mL) columns of the resin or by mixing slurry with 2 volumes of washing buffer and separating the supernatant following centrifugation.

Fluorescent Labeling of Actin. Actin was prepared from an acetone powder of rabbit back and leg muscles (Taylor & Weeds, 1976) and labeled with *N*-(1-pyrenyl)iodoacetamide (purchased from Molecular Probes and used without further purification) as described by Kouyama & Mihashi (1981). F-Actin at 1 mg·mL^{-1} (25 μM) was incubated with *N*-(1-pyrenyl)iodoacetamide (25–30 μM) for 24 h in the dark at 4 °C in 25 mM Tris-HCl, pH 8.2, 100 mM KCl, 1 mM $MgCl_2$, 1 mM ATP, and 3 mM azide. F-Actin was then sedimented for 2–3 h at 100000*g*, and the pellets were suspended in G buffer (2 mM Tris-HCl, pH 8.0, 0.2 mM ATP, 0.2 mM DTT, 10^{-4} M $CaCl_2$, and 1 mM azide) and dialyzed for 2–3 days to depolymerize the actin. Residual filaments were removed by centrifugation at 100000*g*, and the supernatant G-actin was used for polymerization studies or repolymerized in 5 mM $MgCl_2$ and 100 mM KCl for subsequent depolymerization studies. Occasionally preparations were subjected to a second cycle of depolymerization and repolymerization. The extent of incorporation of label into actin was determined by using the molar absorption coefficient for *N*-(1-pyrenyl)iodoacetamide–G-actin of 2.2×10^4 M^{-1} cm^{-1} at 344 nm (Kouyama & Mihashi, 1981) and measuring actin concentration by the method of Bradford (1976) or with the Folin reagent, using unlabeled actin as standard. Actin concentration was also measured by the absorbance at 290 nm by using A_{290} = 0.63 for 1 mg·mL^{-1} actin (Lehrer & Kerwar, 1972). (The fluorophore contributes less than 10% to the absorbance at this wavelength, but no corrections were made for this.) Moles of fluorophore incorporated per mole of actin ranged from 0.6 to 0.9 but were usually 0.8–0.85.

Fluorescence spectral measurements were made by using a Perkin-Elmer MPF-3 spectrofluorometer maintained at 20 °C with a constant-temperature circulating water bath. For fixed-wavelength measurements, the emission wavelength was 384 nm, and excitation wavelengths were 366 nm for F-actin and 344 nm for G-actin. The fluorescence intensities in arbitrary units for both G-actin and F-actin were determined by measurements of fluorescence at increasing concentrations of the two proteins, and critical concentrations were estimated from the intersection of the two slopes. At very low concentrations of actin (less than 20 μg·mL^{-1}), corrections were made for the background fluorescence and Raman emission of the buffers. No corrections were made for self-absorbance of the protein due to "inner filter effects"; even at concentrations of 0.6 mg·mL^{-1}, the absorbance at 344 nm in the 2-mm pathlength cells was only about 0.05. Ratios of fluorescence intensities at excitation wavelengths of 366 and 344 nm were obtained for both G- and F-actin (here termed the spectral ratio). Alternatively, ratios were determined from fluorescence maxima observed in excitation spectra, although it should be noted that there is a slight shift in the absorbance maximum for F-actin from 344 to about 347 nm. During polymerization experiments, the fluorescence was followed continuously for several minutes, though with slow polymerizations (taking 5 min or more), the fluorescence was measured intermittently to avoid overexposing the fluorophore to intense ultraviolet light. Both excitation and emission slits were set at 4 nm.

Viscosity measurements were made in a Cannon-Manning capillary flow viscometer (Model 100) at 20 °C. A volume of 0.6 mL was required to fill the viscometer, which had a flow time for buffer of 83–84.5 s.

UV Difference Spectroscopy. Actin was polymerized at 0.4–1.0 mg·mL^{-1} in buffer containing 0.1 mM ATP in 2- or 5-mm quartz cuvettes. Polymerization was initiated by addition of 2 M KCl and 100 mM $MgCl_2$ to a final concentration of 0.1 M KCl and 5 mM $MgCl_2$ in one cuvette and an equivalent volume of water in the matched cuvette. The increase in absorbance at 232 nm was followed in a Cary 17 spectrophotometer (Varian, Palo Alto, CA) at 21 °C. The difference between A_{232} at time t and the steady-state value attained after polymerization was plotted in a semilog form to obtain the rate of decay of actin monomer, as described by Cooke (1975). No corrections were made for the increase in turbidity on polymerization (Higashi & Oosawa, 1965).

Ca^{2+} Concentration. Ca^{2+}–EGTA buffers were used to regulate free calcium ion concentrations, which were calculated by using the dissociation constants of Harafuji & Ogawa (1980). Standard conditions were 0.1 mM $CaCl_2$ either with or without 0.25 mM EGTA [giving a free calcium concentration in the presence of EGTA of 2.7×10^{-9} M at pH 8 (here written as $<10^{-8}$ M)].

Electron Microscopy. Actin samples were stained with uranyl acetate on carbon-coated grids as described by Craig et al. (1980) and examined by using a Philips 300 or Philips 400 electron microscope. Lengths of actin filaments under different conditions were compared by evaluation of the number-average, $\langle L \rangle_n$, and weight-average, $\langle L \rangle_w$, lengths (Kawamura & Muruyama, 1970). Because we needed to obtain measurements on very short filaments, lengths were measured at a magnification of about 60000×. The minimum length which could be detected was about 0.02 μm. Filaments from control actin samples were too long to fit completely within a single field of 3.0 × 3.75 μm. Thus, values for $\langle L \rangle_n$ and $\langle L \rangle_w$ were determined for all filaments and portions of filaments falling within the field: this will give a considerable underestimate for the true values of these lengths in the control samples. However, the purpose of measuring control preparations was to ensure that no significant spurious fragmentation had occurred, and since the values for the controls were very much greater than those for preparations containing ADF, we did not consider it essential to make measurements over much larger fields.

Polyacrylamide gel electrophoresis in the presence of sodium dodecyl sulfate was carried out in slab gels by using a Tris–Bicine buffer system as described previously (Taylor & Weeds, 1976). Gel overlays were performed by B. Pope by using the conditions of Snabes et al. (1981).

Results

Purity of ADF Preparations. Two alternative procedures were used in the initial stages of ADF preparation. The ammonium sulfate precipitation and DEAE-cellulose chromatography have been described previously (Harris & Gooch, 1981). A very large column has to be used since ADF is not bound but albumin and other major components of plasma are removed on the column. In the second procedure, poly(ethylene glycol) is used in place of ammonium sulfate to remove fibrinogen in the 0–5% fraction (Polson et al., 1964), and ADF is precipitated largely in the 5–15% fraction. This protein binds tightly to carboxymethylcellulose and is eluted with a step to 0.35 M NaCl (see Materials and Methods). The second procedure gave somewhat improved recoveries of ADF and is more rapid to execute. Further purification is then obtained with a second carboxymethylcellulose column by using a salt gradient to improve the separation from immu-

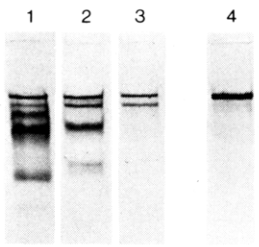

FIGURE 1: Polyacrylamide gel electrophoresis on 7.5% gels in sodium dodecyl sulfate of partially purified and purified pig plasma ADF. (1) ADF after carboxymethylcellulose chromatography; (2) ADF after subsequent hydroxyapatite chromatography: components in order of increasing mobility are ADF, M_r 80000 fragment of ADF, and immunoglobulin heavy chains and light chains; (3) ADF after removal of immunoglobulin by protein A affinity chromatography; (4) different preparation of ADF in which there was no detectable proteolysis.

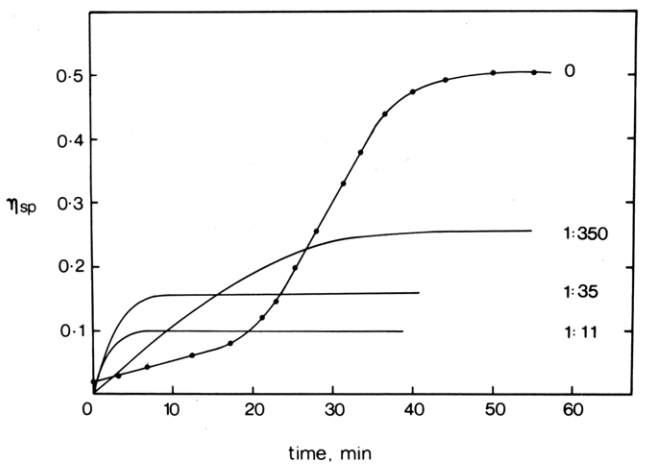

FIGURE 2: Actin polymerization in the presence of variable amounts of ADF followed viscometrically. Actin polymerized at 0.5 mg·mL^{-1} at pH 8.0 in 0.2 mM ATP and 0.1 mM $CaCl_2$ by addition of KCl to 50 mM at zero time. Numbers at right indicate mole ratios of ADF:actin.

noglobulins. Figure 1 shows polyacrylamide gel electrophoresis of two of the preparations of ADF used in these experiments. The major impurity in these preparations is a component of about M_r 80000, which appears to be a fragmentation product of ADF. The extent of contamination by this component was variable, and its presence usually increased during the final purification on hydroxyapatite in spite of attempts to eliminate proteolysis by removal of plasminogen on lysine–Sepharose and by adding both diisopropyl fluorophosphate and leupeptin. In addition, preparations were frequently contaminated by residual immunoglobulins, but the bulk of these could be removed by using protein A–Sepharose affinity chromatography. Because of the presence of these contaminants, an extinction coefficient for the protein has not been determined, and concentrations are based on the DNase inhibition assay as described previously (Harris et al., 1982). The experiments shown in Figures 7–9 were carried out by using the preparation shown in lane 4 of Figure 1, which is free of proteolytic contaminants; most other experiments were carried out with preparations resembling that in lane 3 of Figure 1, which contains a prominent M_r 80000 band.

Actin Polymerization in the Presence of ADF. (*1*) *Viscometric Studies.* When actin in G buffer containing 10^{-4} M calcium polymerizes in KCl but in the absence of magnesium, there is a long lag phase (about 20 min in Figure 2) before the viscosity increases to its equilibrium value. The presence of low molar amounts of ADF (as little as one to a few hundred actins) has two effects: (i) the lag phase is abolished; that is, polymerization is accelerated, but (ii) the final equilibrium

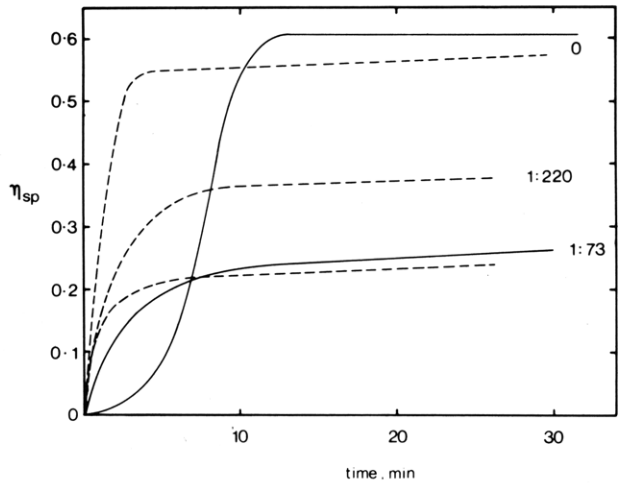

FIGURE 3: Calcium dependence of actin polymerization in the presence of variable amounts of ADF followed viscometrically. Actin polymerized at 0.47 mg·mL^{-1} in 2 mM Tris-HCl, pH 8.0, 0.2 mM ATP, 0.2 mM DTT, 0.1 mM $CaCl_2$, 50 μM $MgCl_2$, and 1 mM azide. (—) No EGTA; (---) 0.25 mM EGTA (Ca^{2+} concentration $<10^{-8}$ M). Polymerization was initiated by addition of KCl to 100 mM.

viscosity is decreased (Figure 2). There is a progressive lowering of the final viscosity with increasing ADF concentration. Figure 3 shows a comparison of these changes in the presence (10^{-4} M) and effective absence ($<10^{-8}$ M) of free Ca^{2+}. In this experiment, a low magnesium concentration was included (50 μM) because G-actin is not stable in the complete absence of divalent cations. It is noteworthy that the final viscosity (after 25 min of reaction time) is almost identical at high and low Ca^{2+} concentrations, although it decreases progressively with increasing ADF concentration in both cases. Thus, ADF decreases the equilibrium viscosity of actin in a Ca^{2+}-independent manner. However, no conclusions can be drawn on the Ca^{2+} sensitivity of the effects of ADF on the *rates* of actin polymerization, because, as is clear from Figure 3, actin polymerization at low magnesium concentrations is markedly accelerated when Ca^{2+} concentration is lowered, even in the absence of ADF. The polymerization rate becomes Ca^{2+} independent only at much higher Mg^{2+} concentrations (see below), and under these conditions, the reaction is too fast to monitor by viscometry.

(*2*) *Polymerization Studies with Fluorescently Labeled Actin.* A more direct measure of actin monomer incorporation into filaments is to follow the change in fluorescence on polymerization of *N*-(1-pyrenyl)iodoacetamide-labeled actin (Kouyama & Mihashi, 1981). This technique also permits monitoring of much more rapid changes than can be followed viscometrically, and it can therefore be used to analyze the effects of ADF on both the rate and extent of actin polymerization. Labeled G-actin has an excitation maximum at 344 nm and an emission maximum at 384 nm. When it assembles into filaments, there is a very large enhancement in fluorescence intensity, and the spectrum shows new peaks: the F-actin spectrum has excitation maxima at 347 and 366 nm, with emission maxima at 384 and 407 nm (Kouyama & Mihashi, 1981). Throughout these experiments, an emission wavelength of 384 nm was used. Thus, the conversion of G-actin into filaments is accompanied both by an increase in the fluorescence intensity at an excitation wavelength of 366 nm and by an increase in the ratio of fluorescence measured at excitation wavelengths of 366 and 344 nm.

Control experiments were carried out to determine the linearity of fluorescence with actin concentration, in both G and F forms, by using excitation wavelengths of 344 and 366

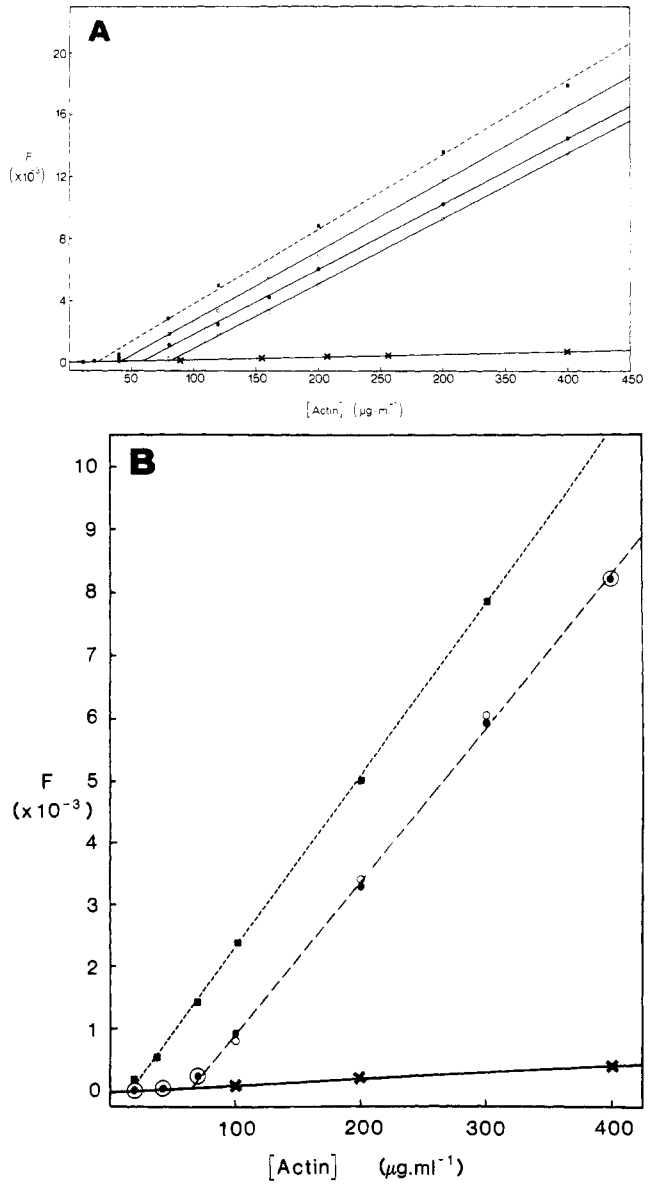

FIGURE 4: Measurement of critical concentration using *N*-(1-pyrenyl)iodoacetamide-labeled actin. (A) Actin was polymerized at the concentrations shown for >5 h at 25 °C in 0.1 M KCl and 5 mM $MgCl_2$ in the absence of ADF (■) or in the presence of 0.02 (□), 0.1 (●), or 0.3 μM ADF (○). (B) Actin polymerized at the concentrations shown for >4 h under similar conditions in the presence of 0.1 μM ADF (●) or in the absence of ADF (■). G-Actin controls (×). The critical concentration of G-actin is at the intersection of the lines. Open circles show the fluorescence of samples of F-actin incubated for similar periods with 0.1 μM ADF.

nm. Fluorescence intensity increased linearly over the concentration range tested (0–0.6 mg·mL^{-1}). The slope of this line is a measure of the fluorescence intensity per microgram per milliter of actin in either G or F forms, and these values were obtained for each preparation of labeled actin. The fluorescence intensity of F-actin is 20–30 times that of G-actin (excitation wavelength 366 nm). This marked difference facilitated measurement of the critical concentration of actin: following polymerization at concentrations between 0.01 and 0.50 mg·mL^{-1} in the appropriate salts for 2–4 h at ambient temperature, there was a steep rise in the fluorescence intensity above the critical concentration (see Figure 4). For actin polymerized in 5 mM $MgCl_2$ and 100 mM KCl, the critical concentration varied between preparations, in the range 0.01–0.03 mg·mL^{-1}. Somewhat higher critical concentrations were obtained for actin polymerized at lower magnesium

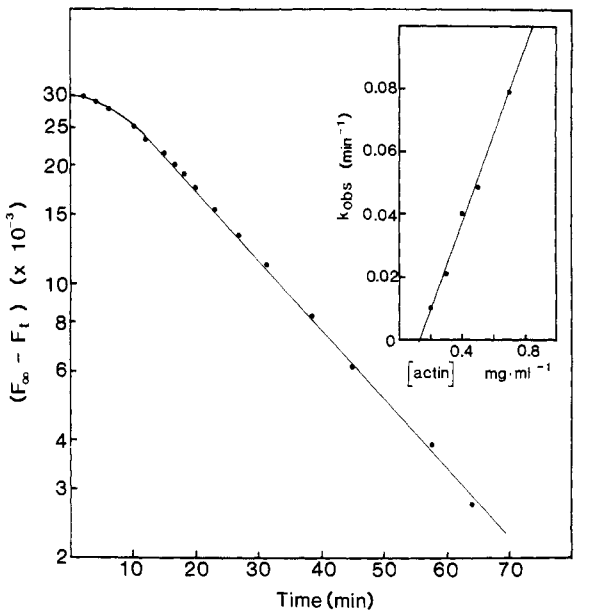

FIGURE 5: First-order plot of the change in fluorescence intensity during the approach to equilibrium ($F_\infty - F_t$) for actin polymerized at 0.4 mg·mL^{-1} by addition of 100 mM KCl and 5 mM $MgCl_2$. Following an initial lag, log ($F_\infty - F_t$) against time is linear, with the slope $-k_{obsd}$. The inset shows the relationship between k_{obsd} and the initial actin concentration.

concentrations. Throughout these experiments at pH 8.0, 5 mM $MgCl_2$ was used because the critical concentration and the observed rates of polymerization were minimally changed when EGTA was added at 0.25 mM to remove the 0.1 mM $CaCl_2$ present in G-actin.

Control experiments also showed an increase in the spectral ratio from about 0.6 for G-actin to about 1.6 maximally for F-actin. These ratios were also determined for each preparation of labeled actin. Taken together, the spectral ratios and the fluorescence intensities at 366 nm for both G- and F-actin can be used to estimate (albeit approximately) the proportion of each in any mixture of the two. Because the fluorescence intensity of F-actin is about 20 times that of G-actin, the F spectrum dominates until the proportion of G-actin is very high. However, when actin is polymerized at concentrations just above the critical concentration, both the fluorescence intensity and the spectral ratio clearly reflect the presence of the monomer.

The rate of actin polymerization was measured by following the fluorescence increase at an excitation wavelength of 366 nm when 0.1 M KCl and 5 mM $MgCl_2$ were added to G-actin. Following an initial short lag period (which diminished as the actin concentration increased), the fluorescence increased exponentially to a maximum value, dependent on actin concentration. Figure 5 shows a semilog plot of the approach to equilibrium against time. The slope of this plot gives the rate constant, k_{obsd}. The inset to Figure 5 shows the linear relationship between these observed rate constants and the initial G-actin concentration.

It is important that the behavior of the fluorescently labeled actin should not be significantly different from that of unlabeled actin preparations. Polymerization of labeled actin showed a similar viscosity rise to unlabeled material. Labeled actin copolymerized with unlabeled actin [see also Pinder & Gratzer (1982)]. The rates of actin polymerization obtained by spectrofluorometry were compared with those from difference UV measurements at 232 nm. Using *N*-(1-pyrenyl)iodoacetamide-labeled actin undiluted, we found that the spectral properties of the attached fluorophore interfered with

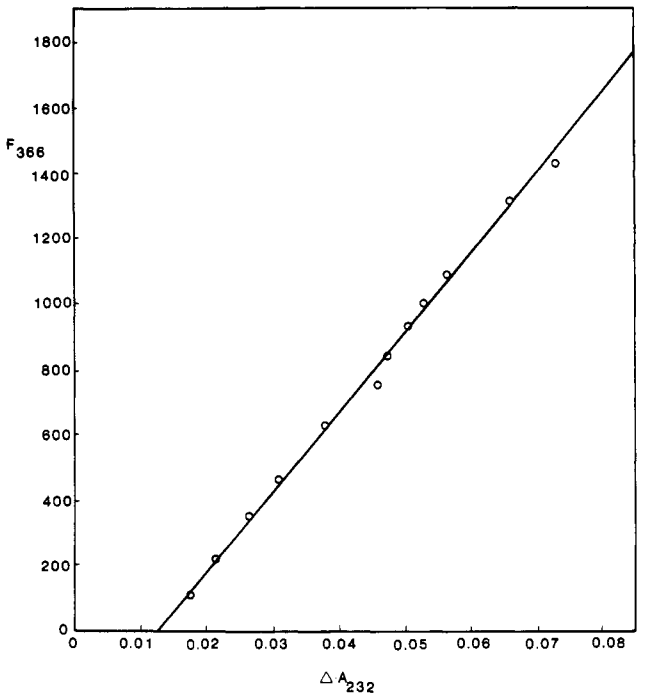

FIGURE 6: Increase in fluorescence at 366 nm correlated with the increase in absorbance at 232 nm for *N*-(1-pyrenyl)iodoacetamide-labeled actin polymerized in the presence of 0.1 M KCl and 5 mM $MgCl_2$. Samples of actin (containing labeled:unlabeled monomers in the ratio 1:20) were polymerized at 1.0 mg·mL^{-1} final concentration. The increase in fluorescence is compared to the increase in the difference absorbance over a 40-min period.

the protein difference spectrum, but these problems were virtually eliminated by copolymerizing the labeled monomers in the presence of a 20-fold excess of unlabeled G-actin. Figure 6 shows that the fluorescence increases linearly with increasing absorbance at 232 nm during a 40-min polymerization reaction (samples taken from the same solution polymerized under identical conditions over the same time period). Rate constants obtained from semilog plots by either method were in good agreement (e.g., actin polymerized in the absence of ADF gave an observed rate of 0.377 min^{-1} by UV difference spectroscopy and 0.388 min^{-1} by spectrofluorometry). Similar agreement was obtained for polymerization reactions carried out in the presence of ADF. Thus, fluorescence enhancement correlates directly with the change in absorbance at 232 nm that occurs on actin polymerization. (It was also established by using unlabeled actin that the increase in light scattering occurring on actin polymerization did not interfere with the fluorescence signals at the wavelengths used.)

Similar exponential curves were obtained when G-actin was polymerized in the presence of ADF. Full excitation spectra (emission at 384 nm) were run both before polymerization and at the completion of polymerization to ensure that the observed increase in intensity at a single wavelength corresponded to a change from a G-type to an F-type spectrum. ADF has the following three effects: (i) it decreases the initial lag period preceding the exponential rise in fluorescence; (ii) it enhances the rate of this exponential phase; (iii) it diminishes the magnitude of the total fluorescence change. In one experiment, in which the k_{obsd} for polymerization (under the conditions of Figure 9) was 0.064 min^{-1} both with and without calcium, ADF at a molar ratio of 1:22 actin monomers substantially increased k_{obsd} to 1.6 min^{-1} in 10^{-4} M calcium but to only 0.18 min^{-1} at $<10^{-8}$ M calcium. Thus, the ADF-induced acceleration of actin assembly is strongly calcium sensitive. Qualitatively similar results were obtained at pH 7–8.5 and

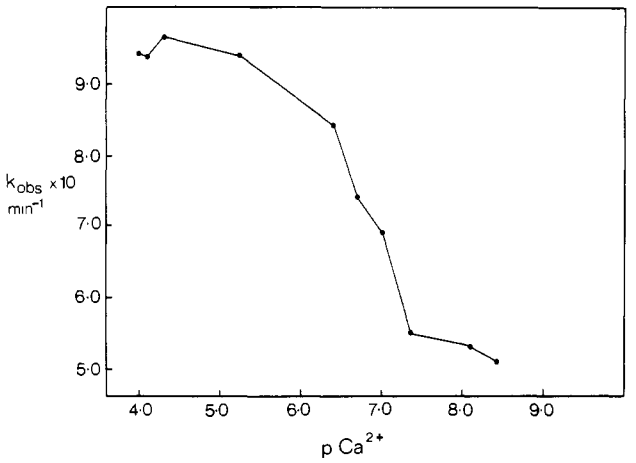

FIGURE 7: Calcium dependence of the rate of *N*-(1-pyrenyl)iodoacetamide-labeled G-actin polymerization with plasma ADF. Actin at 0.2 mg·mL^{-1} (4.8 μM), with 0.22 μM ADF, in 2 mM sodium phosphate, pH 7.0, 0.2 mM ATP, 0.2 mM DTT, 0.1 mM $CaCl_2$, and variable EGTA concentrations was polymerized by addition of KCl to 100 mM and $MgCl_2$ to 5 mM.

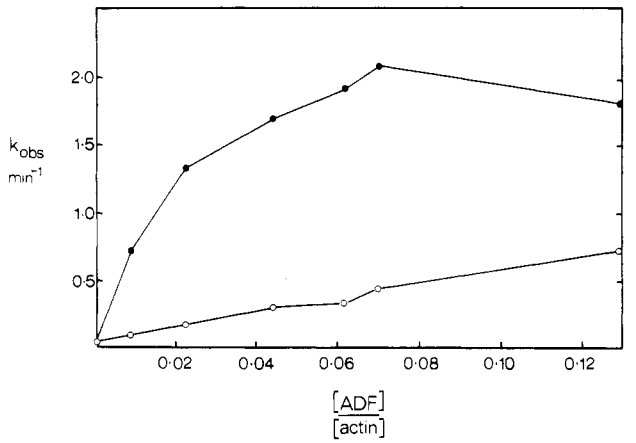

FIGURE 8: Dependence of the polymerization rate, k_{obsd}, of *N*-(1-pyrenyl)iodoacetamide-labeled actin on ADF concentration. Actin at 0.2 mg·mL^{-1} in 5 mM Tris-HCl, pH 8, 0.2 mM ATP, and 0.2 mM DTT was polymerized by addition of KCl to 100 mM and $MgCl_2$ to 5 mM: 10^{-4} M free Ca^{2+} (●); $<10^{-8}$ M free Ca^{2+} (○).

at lower (1 mM) $MgCl_2$ concentrations. Although the ratio of the observed rate in the presence of calcium to that in its absence was greater at pH 8 than at pH 7, calcium dependence was measured at pH 7, because EGTA controls the free calcium concentration to a higher value at this pH. Figure 7 shows that k_{obsd} declines most steeply between about 10^{-6} and 10^{-7} M Ca^{2+}, i.e., in the range of physiological intracellular calcium. By contrast, control actin in the absence of ADF shows an increase in k_{obsd} with decreasing Ca^{2+} concentration at pH 7.0: k_{obsd} was 0.13, 0.28, and 0.38 min^{-1} at 10^{-4}, 2×10^{-7}, and 4×10^{-9} M free Ca^{2+}, respectively. (These rates are all lower than those observed in the presence of ADF.) The calcium dependence illustrated in Figure 7 is therefore due to the influence of ADF on actin polymerization and is not a property of actin alone.

The dependence of k_{obsd} on ADF concentration, at both high and low calcium concentrations, is shown in Figure 8. At low Ca^{2+} concentration ($<10^{-8}$ M), k_{obsd} increases approximately linearly with ADF concentration, implying a simple dependence on the number of ADF molecules present. [The extent of this increase in rate was variable, but in two sets of experiments (one shown in Figure 8), it was 3- and 7-fold at ADF:actin ratios of about 1:7.] At 10^{-4} M Ca^{2+}, k_{obsd} increases

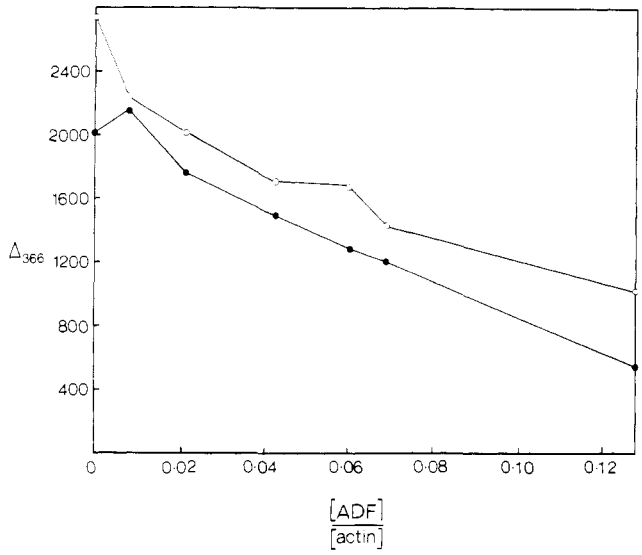

FIGURE 9: Fluorescence change of *N*-(1-pyrenyl)iodoacetamide-labeled actin on polymerization: dependence on plasma ADF. Actin at 0.2 mg·mL^{-1} in 5 mM Tris-HCl, pH 8.0, 0.2 mM ATP, and 0.2 mM DTT was polymerized by addition of KCl to 100 mM and $MgCl_2$ to 5 mM. The ordinate is the total fluorescence intensity change in arbitrary units; excitation at 366 nm, emission at 384 nm: 10^{-4} M free Ca^{2+} (●); $<10^{-8}$ M free Ca^{2+} (○).

much more rapidly with ADF concentration to a plateau, where the rate constant is 35–40 times that in the absence of ADF. Under these saturating conditions, polymerization as defined by the fluorescence increase is no longer dependent on ADF concentration but may be controlled instead by limiting actin concentration. [In an experiment similar to that of Figure 8, but at twice the actin concentration (0.4 mg·mL^{-1}), k_{obsd} continued to increase beyond the plateau observed at 0.2 mg·mL^{-1} actin.] Limited data prevent a full quantitative analysis at this stage, but it seems probable that the rate constant is limited either by ADF or by free actin monomer concentration, depending on the ratio of ADF to actin.

A further complication at very high ratios of ADF to actin (>1:20) is that the fluorescence change is biphasic. Initially, the signal increases exponentially to a maximum, in about 2–3 min, and this curve is used to calculate k_{obsd}. However, the maximum fluorescence is not maintained (as it is at lower ratios of ADF to actin in the presence of calcium and in all cases in EGTA) but declines over about 10 min to an equilibrium value, which is about 80% of the maximum level. This suggests that, in addition to the fluorescence increase observed during polymerization, there is a decline in fluorescence due to a second and slower process. This second phase in the fluorescence profile could be caused either by a reduction in the fluorescence yield of the labeled F-actin due to conformational changes or by a reequilibration of the actin toward the monomer (or a fluorescent species like the monomer) (see Discussion).

Experiments were also carried out to examine the fluorescence change when actin was polymerized in the presence of ADF at molar ratios of between 1:1 and 4:1 by using ADF concentrations of about 2 μM. There was no significant enhancement of fluorescence at ADF:actin ratios of 1:1 or 1:2, but at ratios of 1:3 and 1:4, the enhancement was 2–4-fold. These results suggest that there is no increase in actin fluorescence until at least three actin monomers are bound to ADF.

The total fluorescence change declines with increasing ADF concentration at both high and low Ca^{2+} concentrations as shown in Figure 9. (At high ADF concentrations, the fluorescence intensity change plotted is the equilibrium, rather than the maximum value as described above; the difference of about 20% between these two measurements does not significantly affect the shape of the plot.) Thus, the equilibrium fluorescence of actin polymerized in the presence of ADF (like the equilibrium viscosity) shows little dependence on Ca^{2+} concentration; this contrasts with the marked Ca^{2+} sensitivity in the *kinetics* of the fluorescence change.

The increase in fluorescence on actin polymerization is accompanied by a change from a G-actin to an F-actin spectrum. The initial excitation spectra for all the experiments of Figures 8 and 9 had intensity ratios for 366:344 nm (emission at 384 nm) of 0.71 ± 0.03, characteristic of G-actin: under these conditions, ADF has no significant effect on the spectral properties of G-actin. After polymerization, the 366:344 nm ratio was 1.42 in the absence of ADF (with and without Ca^{2+}), characteristic of F-actin, but the ratio declined with increasing ADF concentration to 1.08 (high Ca^{2+} concentration) and 1.27 (low Ca^{2+} concentration) at 1 ADF per 7.7 actins. This observation implies that a greater proportion of the actin is G-like in its spectral characteristics in the presence of ADF.

One way to demonstrate an increase in actin monomer concentration after polymerization in the presence of ADF is to measure the critical concentration with and without ADF but under otherwise identical conditions. Figure 4 shows that the apparent critical concentration is considerably higher in the presence of ADF: it increased from about 20 μg·mL^{-1} in the absence of ADF to 63 μg·mL^{-1} in the presence of 0.1 μM ADF (mean of two experiments shown in Figure 4A,B). [Values of 54 and 83 μg·mL^{-1} were obtained at 0.02 and 0.3 μM ADF, respectively (Figure 4A).] Polymerization experiments carried out at 10^{-4} M Ca^{2+} or at $<10^{-8}$ M Ca^{2+} in the presence of ADF gave similar critical concentrations. The increases in critical concentration estimated by this method are consistent with the decline in fluorescence observed in polymerization experiments as shown in Figure 9. However, it should be noted that these apparent critical concentrations reflect the presence not only of G-actin but also of complexes with ADF that have fluorescence properties like those of G-actin.

[If addition of ADF affects only the equilibrium between fluorescent forms of G- and F-actin, the slopes of the lines in Figure 4 (representing the fluorescence intensity per microgram of F-actin) should be identical. In practice, the slope decreases with increasing ADF concentration about 10% overall. This does not reflect the "assembly competence" of the actin, since denatured material should be identical in all cases. The most likely explanation for this change in slope is that a bias has been introduced through incorporation of data points at low actin concentrations where the slope is changing in an upward direction from the G to the F state and a further downward bias at high actin concentrations where self-absorption becomes significant. Measurements made at even higher actin concentrations (up to 1 mg·mL^{-1}) showed that the incremental fluorescence intensity was lower than expected by extrapolation.]

To check that the fluorescence enhancement was indeed due to filament assembly, small samples were removed from the polymerized ADF–actin mixtures of the experiments of Figures 8 and 9, placed on electron microscope grids, and negatively stained with uranyl acetate. ADF increased the proportion of shorter filaments both at 10^{-4} M and at $<10^{-8}$ M calcium. Thus, the lower fluorescence intensity observed in the presence of ADF correlates both with the formation of shorter filaments

and with an increase in the G-actin concentration.

Similar polymerization experiments were carried out in the presence of human ADF, with actin at 0.2 mg·mL^{-1} and ADF:actin in the range 1:900 to 1:16. The rate constant increased linearly from 0.038 min^{-1} in the absence of ADF to 1.34 min^{-1} at the highest ADF:actin ratio in the presence of 0.1 mM calcium, but there was negligible effect on the rate constant at $<10^{-8}$ M calcium (k_{obsd} = 0.039 min^{-1} at ADF:actin = 1:33). However, as in the experiments with pig ADF, the final fluorescence intensity was markedly decreased even in low calcium concentration.

Calcium Sensitivity of ADF Binding to the DNase–Actin Complex. Plasma ADF binds specifically and tightly to actin-saturated DNase I that has been covalently coupled to Sepharose (Harris & Gooch, 1981). A variety of elution conditions were tested by a rapid sedimentation assay, and both eluted products and residual protein were analyzed by polyacrylamide gel electrophoresis in the presence of sodium dodecyl sulfate. The following conditions did not elute either ADF or actin: buffers containing 5 mM EGTA at pH 7.0 (free Ca^{2+} $<10^{-8}$ M); KCl, KI, or KCNS at 1 M; various buffers in the pH range 2–10 (0.2 M); excess free G-actin (4 mg·mL^{-1}); 10^{-6} M cytochalasin B; 20% formamide; or urea at ≤4 M. Both ADF and actin were eluted with denaturing agents including 40% formamide (Zechel, 1980), urea at ≥6 M, or 3 M guanidine hydrochloride. Thus, these experiments failed to identify any conditions which would specifically release ADF from the DNase–actin complex.

It has been reported that rabbit serum brevin, like villin, elutes from DNase–actin at low calcium concentrations (Harris & Schwartz, 1981), and Thorstensson et al. (1982) have purified human serum ADF under similar conditions. Further attempts were therefore made to elute ADF with EGTA-containing buffers by using small columns. Eluted protein was only a very small fraction of the total amount on the column; 5 mM EGTA, 0.15 M NaCl, 1 mM dithiothreitol, and 20 mM Tris-HCl, pH 7.8 (Bretscher & Weber, 1980), eluted about 15% of the total protein (but not more than 10% of the total ADF). Other experiments were carried out in which ADF saturated with G-actin in solution was applied to a DNase–Sepharose column, rather than a column presaturated with actin, but, again, in no case was there specific recovery of ADF in the absence of actin in the EGTA-containing eluate. In conclusion, we have consistently been unable to purify ADF from actin which is noncovalently bound to DNase–Sepharose. This confirms other results presented in this paper that ADF binds tightly to actin in a calcium-insensitive manner.

Effect of ADF on Preformed Actin Filaments. (1) Viscometric Studies. ADF decreases the viscosity of actin filaments (Figure 10). The viscosity declines particularly steeply with increasing ADF concentration at ADF:actin ratios up to 1:100, reaching a minimum value at about 1:20. Quantitatively similar changes in viscosity occur at both high (10^{-4} M) and low ($<10^{-8}$ M) free calcium concentrations. The changes effected by ADF are very much greater than those obtained by dilution of the sample by equivalent volumes of buffer.

(2) Studies with Fluorescently Labeled Actin. *N*-(1-Pyrenyl)iodoacetamide-labeled actin was also used to investigate the effect of ADF on actin filaments. These experiments were performed under two sets of contrasting conditions, because it seemed likely that the response of actin to ADF might be influenced by solution conditions that could promote or inhibit free exchange of monomers at filament ends. Filaments were therefore titrated with ADF either in 15% glycerol in the absence of ATP, where they are stable (Harris et al., 1982), or in 0.2 mM ATP, where they are expected to be in dynamic equilibrium with monomers (Wegner, 1976; Simpson & Spudich, 1980; Wegner & Neuhaus, 1981). (Because filaments might be susceptible to irreversible mechanical breakage during mixing, resulting in artifactual "depolymerization", controls were carried out in which F-actin was mixed vigorously with a Pasteur pipet, with or without buffer addition. Spectrofluorometric analysis immediately after this agitation did not give a significant decrease in fluorescence.)

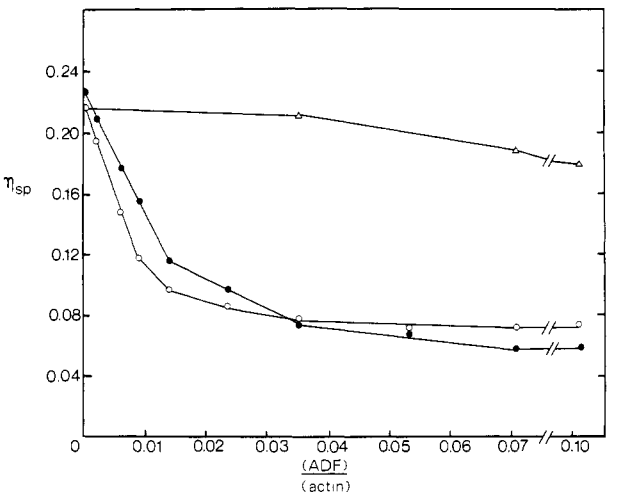

FIGURE 10: Effect of human plasma ADF on the high shear viscosity of F-actin. F-Actin at 0.2 mg·mL^{-1} in 20 mM Tris-HCl, pH 8.0, 0.2 mM ATP, 0.2 mM DTT, 1 mM azide, 5 mM $MgCl_2$, 100 mM KCl, and 10^{-4} M $CaCl_2$ was titrated with increasing amounts of human plasma ADF in 10^{-4} M free Ca^{2+} (●) and $<10^{-8}$ M free Ca^{2+} (○). The fall in viscosity on each ADF addition was not instantaneous: repeated determinations were made until a stable minimum was reached (5–10 min). Control additions of buffer without ADF (in 10^{-4} M Ca^{2+}) (△).

The titration of glycerol-stabilized F-actin with ADF is shown in Figure 11A. Each addition of ADF gave a drop in fluorescence within the mixing time, and the fluorescence intensity declined approximately linearly with increasing ADF concentration. The fluorescence intensity was reduced to that of G-actin at an ADF:actin ratio of about 0.5. There was no qualitative difference between the titrations at high and low Ca^{2+} concentrations, but slightly higher ADF concentrations were needed to give quantitatively the same fluorescence change at low Ca^{2+} concentration. When these titrations were complete, the actin spectra were comparable to those of the free monomer: the 366:344 nm ratios were both about 0.70.

Figure 11B shows the relationship between the spectral ratio and the fluorescence intensity throughout these experiments. Small additions of ADF at the beginning of the titrations produced a large percentage decrease in fluorescence intensity, while the spectral ratio showed a significant change only toward the end of the titration. Using values for the fluorescence intensity of both G- and F-actins at 344- and 366-nm excitation wavelengths, we have drawn a theoretical curve in Figure 11B that relates the changes in the spectral ratio with the decrease in fluorescence intensity. The observed data points fit closely to the theoretical curve. Comparable plots for the titration of F-actin with ADF in ATP (not shown) were almost superimposable with those of Figure 11B, despite the fact that smaller amounts of ADF were required to produce these spectral changes (see Figure 12).

When a solution of F-actin in ATP was titrated with successive small aliquots of ADF, there was a more complex pattern of fluorescence changes (Figure 12). Three distinct

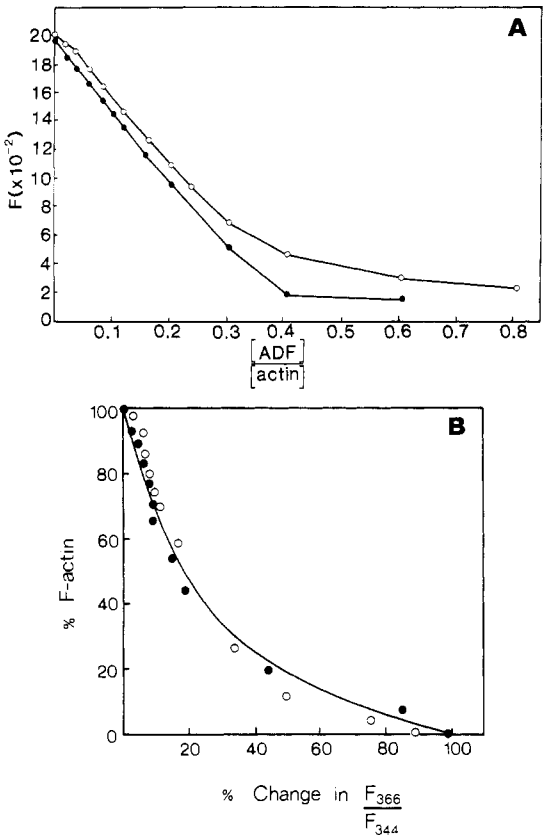

FIGURE 11: Addition of pig plasma ADF to *N*-(1-pyrenyl)iodoacetamide-labeled actin filaments under stabilizing conditions. (A) Fluorescence intensity decrease (excitation at 366 nm and emission at 384 nm) with increasing ADF concentration: actin at 0.1 mg·mL^{-1} in 5 mM Tris-HCl, pH 8.0, 100 mM KCl, 5 mM $MgCl_2$, 0.2 mM DTT, 1 mM azide, and 15% glycerol. 10^{-4} M free Ca^{2+} (●); $<10^{-8}$ M free Ca^{2+} (○). (B) Relationship between the change in the fluorescence spectral ratio (at 366:344 nm excitation, shown as the percent maximum change on the abscissa) and the decline in intensity of fluorescence at 366-nm excitation (expressed as the percent F-actin on the ordinate). Emission wavelength was 384 nm. 10^{-4} M free Ca^{2+} (●); $<10^{-8}$ M free Ca^{2+} (○); the solid line shows the expected relationship if the fluorescence changes were due to the conversion of F-actin to G-actin.

stages occurred in the titration when carried out in 10^{-4} M Ca^{2+}. At ADF:actin ratios of 1:30–1:10, each ADF addition produced a fast (i.e., within a few seconds) drop in fluorescence (vertical arrows in Figure 12) followed by a slow decrease, which took 5–10 min to reach equilibrium. Closely similar changes occurred in experiments at $<10^{-8}$ M Ca^{2+}. Between ratios of 1:10 and 1:5, ADF addition produced a fast drop in fluorescence as before, but the fluorescence then slowly rose to equilibrium (note that the points rise above the lowest point on the vertical arrows). This behavior was never observed at low ($<10^{-8}$ M) Ca^{2+} concentration (Figure 12B). Under these conditions, the pattern of fast followed by slow decrease continued. In the final phase of the titration at ratios of 1:5–1:1.3, the fluorescence changes were small and almost instantaneous. By this stage, the fluorescence excitation spectrum resembled that of G-actin: the 366:344 nm spectral ratio was between 0.7 and 0.8 irrespective of the calcium concentration.

During the course of these ADF additions, the actin was diluted about 25%, and although the fluorescence intensities were corrected for dilution of the labeled actin, this dilution would be expected to product additional actin depolymerization to reestablish the critical monomer concentration. As a control, actin at the same concentration of 0.1 mg·mL^{-1} was titrated

Table I: Actin Filament Length in the Presence and Absence of ADF[a]

conditions	n	$\langle L\rangle_n$ (μm)	$\langle L\rangle_w$ (μm)	$\langle L\rangle_w/\langle L\rangle_n$	field size (μm^2)
Ca^{2+}, polymerization	183	0.075	0.162	2.16	1.7 × 1.53
EGTA, polymerization	218	0.070	0.163	2.33	1.7 × 1.36
Ca^{2+}, depolymerization	212	0.070	0.150	2.14	2.13 × 1.53
EGTA, depolymerization	232	0.077	0.141	1.83	1.62 × 1.43
control, no ADF,	38	0.86	1.51	1.76	3.75 × 3
Ca^{2+}	67	1.68	3.11	1.85	7.5 × 6
control, no ADF,	68	1.03	2.16	2.10	4.25 × 3.4
EGTA	89	1.58	2.96	1.87	9.2 × 7.4

[a] Polymerization experiments: ADF was mixed with G-actin (0.2 mg·mL^{-1}) at a 1:20 mole ratio in 5 mM Tris-HCl, pH 8.0, 0.2 mM ATP, 0.2 mM DTT, and 0.1 mM $CaCl_2$, with or without 0.25 mM EGTA. Polymerization was then initiated by addition of $MgCl_2$ to 5 mM and KCl to 100 mM. Depolymerization experiments: ADF was mixed with F-actin (0.2 mg·mL^{-1}) at a 1:20 mole ratio in 20 mM Tris-HCl, pH 8.0, 0.2 mM ATP, 0.2 mM DTT, 5 mM $MgCl_2$, 100 mM KCl, and 0.1 mM $CaCl_2$, with or without 0.25 mM EGTA. Samples were incubated for several hours at 20 °C, diluted to 50 μg·mL^{-1} actin, placed immediately on carbon film grids, and negatively stained with 1% uranyl acetate.

with buffer in place of ADF. This reduced the fluorescence intensity to 78% of the value expected on the basis of dilution, indicating some additional actin depolymerization. (This control is to be compared to 8.7% of the initial value produced by addition of ADF in 10^{-4} M Ca^{2+} and 13% in $<10^{-8}$ M Ca^{2+}. In other experiments at 0.2 mg·mL^{-1} actin, dilution to 70% of the initial concentration produced a decrease in fluorescence only 6% greater than that expected by dilution of the fluorophore.) It is therefore clear that the bulk of the fluorescence change is caused by the addition of ADF.

Similar experiments were carried out by using human ADF which showed a pattern of behavior identical with that for pig ADF in both 10^{-4} and $<10^{-8}$ M Ca^{2+}. One additional feature is apparent in Figure 12C: at very low ratios of ADF:actin (1:500–1:50, a range not tested with pig ADF), the fluorescence intensity was steady for several minutes following the initial rapid decrease. In this early phase of the reaction, the decline in fluorescence was approximately linear with added ADF and independent of the calcium concentration.

Titrations of fluorescently labeled F-actin with ADF thus show that complete depolymerization of actin (conversion to a species with a monomer-like spectrum) occurs at ADF to actin ratios around 0.6, independently of Ca^{2+} concentration.

Experiments were carried out to measure the critical concentration by mixing F-actin at different concentrations with ADF and measuring the fluorescence at the end of the reaction. As shown in Figure 4B, the fluorescence intensity was identical with that attained when actin was polymerized under the same conditions in the presence of ADF. Thus, the equilibrium position of the fluorescence intensity appears to be the same in both polymerization and depolymerization conditions, giving an identical critical concentration for G-actin. (Data are shown only at 0.1 μM ADF, but experiments at 0.03 and 0.3 μM ADF gave similar agreement.)

Effects of ADF on Filament Lengths. Actin filament lengths progressively shortened as the ratio of ADF to actin was increased. In one experiment to show that filament length decreases with increasing ADF:actin ratios, the number-average length at equilibrium ($\langle L\rangle_n$; Kawamura & Maruyama, 1970) decreased in the ratio 5:2.5:1 when the proportion of ADF was increased in the ratio 1:3:10. (Exact stoichiometries

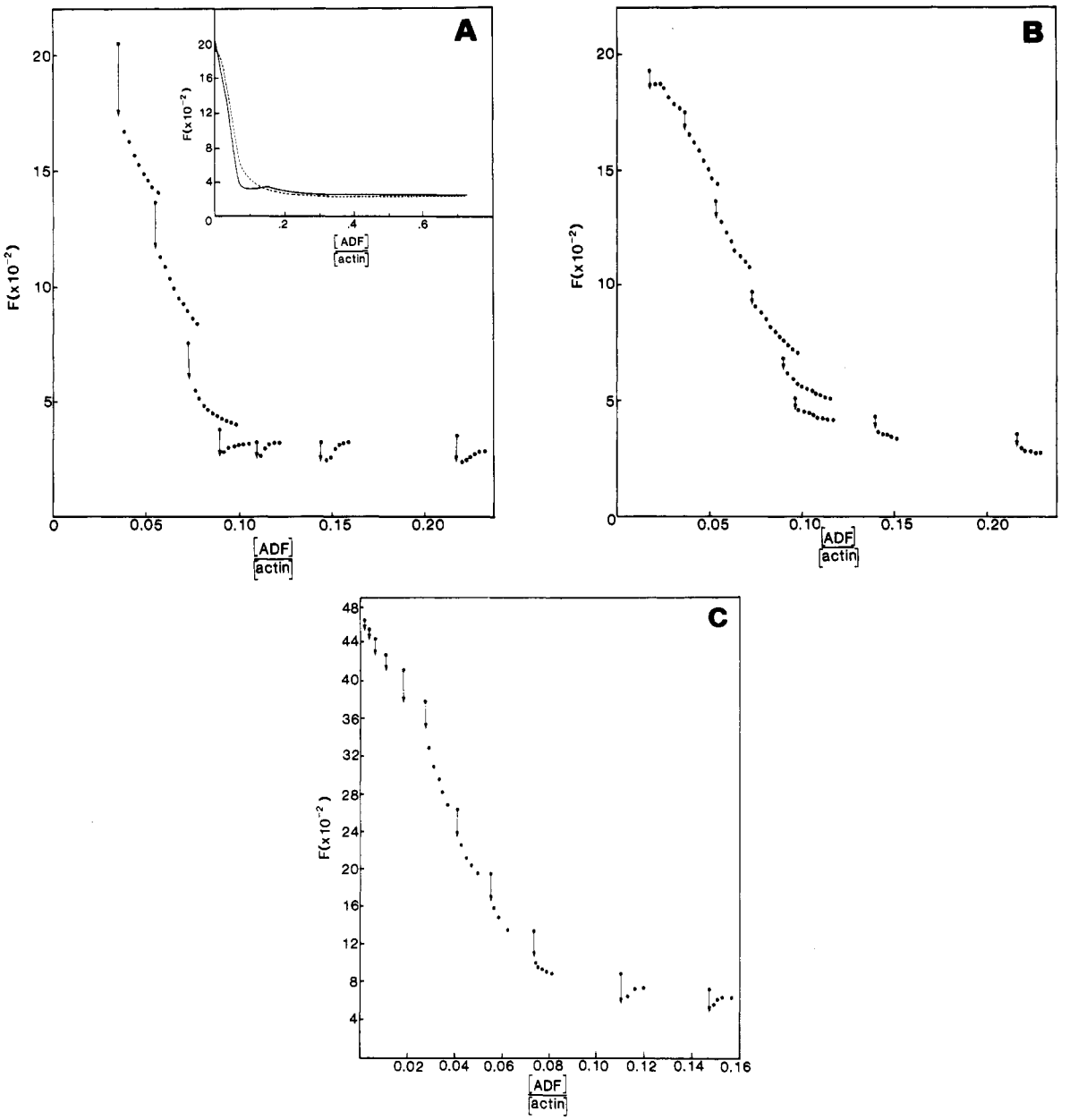

FIGURE 12: Addition of ADF to *N*-(1-pyrenyl)iodoacetamide-labeled actin filaments under conditions allowing spontaneous disassembly. (A) F-Actin at 0.1 mg·mL^{-1} titrated with pig plasma ADF in 5 mM Tris-HCl, pH 8.0, 0.2 mM ATP, 0.2 mM DTT, 1 mM azide, 5 mM $MgCl_2$, 100 mM KCl, and 10^{-4} M free Ca^{2+}. Vertical arrows indicate the magnitude of the fast fluorescence drop at each ADF addition, while subsequent slow changes are indicated by dots at 1-min intervals. The inset shows a comparison of the fluorescence at equilibrium after each ADF addition: 10^{-4} M free Ca^{2+} (—); $<10^{-8}$ M free Ca^{2+} (---). (B) F-Actin at 0.2 mg·mL^{-1} titrated with pig plasma ADF in $<10^{-8}$ M free Ca^{2+}; buffer conditions as in (A). (C) F-Actin at 0.2 mg·mL^{-1} titrated with human plasma ADF in 10^{-4} M free Ca^{2+}; buffer conditions as in (A). In panels A–C, the ordinate is fluorescence intensity in arbitrary units; excitation, 366 nm; emission, 384 nm.

were not determined in this experiment.) In a more extensive survey, the effects of Ca^{2+} concentration on filament length were tested at an ADF:actin ratio of 1:20 (Table I). It is clear that at equilibrium (i.e., after several hours' incubation) there was little difference in length between filaments at high or low free calcium concentration. The capacity of ADF to shorten actin filaments is therefore calcium insensitive. Furthermore, filaments formed by actin polymerization in the presence of ADF were not significantly different in length from those formed by addition of ADF to F-actin. $\langle L \rangle_n$ was in the range 0.07–0.077 μm for all four conditions. [The expected length for a filament of 20 actin monomers is 0.055 μm, based on a double helix with monomer repeat of 54.6 Å (Huxley & Brown, 1967).] Control filaments were more than an order of magnitude longer. (Table I shows that the apparent length of the controls is restricted by the size of field chosen.) The lengths of filaments in all cases were heterogeneous; the ratios of the weight-average to number-average lengths of about 2 are consistent with an exponential length distribution (Kawamura & Maruyama, 1970).

Discussion

In this paper, we have described experiments to investigate the properties of plasma ADF by using a new and sensitive assay for actin polymerization and depolymerization. The results are supported by other methods including viscometric and binding assays and electron microscopy. The main conclusions are the following: (i) ADF shortens and depolymerizes F-actin independently of calcium concentration; (ii) it accelerates actin polymerization in both the absence and presence of calcium, but the enhancement of rate is much greater (about 10-fold) at 10^{-4} M than at $<10^{-8}$ M calcium; (iii) it causes

a progressive increase in the apparent critical concentration as measured by fluorescence under both disassembly and assembly conditions; (iv) ADF binds tightly to actin which is noncovalently linked to Sepharose–DNase and cannot be eluted from the actin in buffers containing $<10^{-8}$ M calcium. These results show that the action of ADF on actin filaments is calcium independent—a conclusion that is at variance with published reports elsewhere both on plasma ADF (Thorstensson et al., 1982) or serum brevin (Harris & Schwartz, 1981) and on related proteins including macrophage gelsolin (Yin et al., 1980, 1981b) and platelet M_r 90 000 protein (Wang & Bryan, 1981). It is important, therefore, to establish that the calcium-dependent and calcium-independent activities of ADF are due to the M_r 92 000 polypeptide and not the consequence of partial proteolytic fragmentation. In addition, it is equally important to show that these properties are attributable to a native protein that has not been prepared under denaturing conditions (e.g., by elution from polyacrylamide gels run in the presence of sodium dodecyl sulfate). The purification procedures described here are carried out under benign conditions and at 4 °C. The major problem in the purification is proteolysis, which becomes serious only at the final stage of hydroxyapatite chromatography with the production of a fragmentation product of about M_r 80 000. However, the preparation of ADF used in the experiments shown in Figures 7–9 contained no detectable breakdown product, and this preparation clearly exhibits calcium-sensitive nucleation; it also reduces actin fluorescence in a calcium-independent manner and increases the critical concentration. Experiments using Sepharose–DNase–actin also confirm that the M_r 92 000 polypeptide binds very tightly to actin in a calcium-independent manner. In addition, gel overlay experiments have been carried out with samples of the M_r 92 000 protein eluted from polyacrylamide gels and iodinated actin under conditions described by Snabes et al. (1981), and these showed that labeled actin bound to the M_r 92 000 protein in both the presence and absence of calcium, though the binding appeared to be much weaker at low calcium concentrations because the radioautographs were consistently weaker at $<10^{-8}$ M calcium (B. Pope, unpublished experiments). Similar results have been obtained in this laboratory for the platelet M_r 90 000 protein which are in full agreement with those published by Snabes et al. (1981).

Because many of the ADF preparations used for these experiments contained variable contamination by a fragment of M_r 80 000, experiments have been carried out to examine the binding of iodinated ADF (containing in addition this proteolytic fragment) to actin by using a sedimentation assay. Preliminary results show that the fragment binds to F-actin in the presence of calcium and is sedimented at 100000*g*, but at $<10^{-8}$ M calcium, it is partially released into the supernatant (B. Pope and A. G. Weeds, unpublished experiments). It should be noted that although actin binding is readily detected for both ADF and the M_r 80 000 fragment by using these methods, the DNase inhibition assay shows a progressive decrease in inhibitory activity in preparations which have lost the M_r 92 000 protein. We therefore believe that the dual calcium-dependent and calcium-independent properties attributed to ADF in this work are not artifacts of proteolytic activity but true activities of the M_r 92 000 protein.

A number of methods have been used to examine the effects of proteins like gelsolin, villin, or ADF on F-actin [reviewed by Schliwa (1981), Pollard & Craig (1982), Korn (1982), and Weeds (1982)]. These include viscometry, sedimentation, and electron microscopy to monitor changes in filamentous actin and DNase inhibition to estimate G-actin. Here we have used a fluorescent probe which, when attached to actin, is exquisitely sensitive to the polymerization state. The method has many advantages. The fluorescence signals are large so that very small concentrations of labeled actin can be used. Unlike difference absorbance measurements at 232 nm, where the signal change on actin polymerization relative to the total absorbance is very small, there is a greater than 20-fold enhancement of fluorescence when labeled actin is polymerized [as shown originally by Kouyama & Mihashi (1981)]. Measurements can be made in the presence of high concentrations of ATP or buffers that interfere with the absorbance at 232 nm. We have shown that the labeled actin provides a useful means of measuring the critical concentration in a very sensitive manner without centrifugation (Figure 4) [see also Pinder & Gratzer (1982)]. However, there is one important caveat which must be stated in any interpretation of fluorescence data in terms of molecular models. Kouyama & Mihashi (1981) have shown clearly that the changes occurring on polymerization of G-actin are reversed by adding myosin subfragment 1 to F-actin. Thus, a change in actin fluorescence may arise through polymerization or depolymerization reactions, or alternatively, it may occur by binding another protein, or indeed by any conformational changes that affect the fluorescence yield. For this reason, it is important to show that the fluorescence changes can be correlated with other methods that measure actin polymerization.

Kinetic analysis of polymerization has been carried out empirically by using semilog plots as described earlier by Cooke (1975) for difference absorbance measurements. As shown in Figure 5, the fluorescence increases, following an initial lag period, to a maximum in an approximately exponential manner and can therefore be analyzed by using the same empirical approach. Furthermore, there is a linear relationship between the fluorescence increase and the change in absorbance at 232 nm as shown in Figure 6, and rate constants obtained by both methods are in good agreement. Pardee & Spudich (1982) have recently shown that the kinetics of actin assembly by rapid sedimentation agree closely with difference absorbance measurements. Thus, fluorescence enhancement appears to be a valid means to estimate the kinetics of actin filament formation. [Since this paper was first submitted, Tellam & Frieden (1982) have shown that the fluorescence enhancement on polymerization is also correlated with F-actin production by using sedimentation.]

The mechanism of actin polymerization is still unclear, but a number of different intermediates have been postulated. Kasai et al. (1962) suggested that the formation of a nucleating species containing three to four actin monomers was rate limiting while elongation occurred very rapidly. The lag phase in polymerization as shown in Figure 5 may correspond to this slow initial production of nuclei. Addition of ADF eliminates this lag phase. F-Actin fragments and complexes with spectrin have been shown markedly to accelerate actin polymerization (Gordon et al., 1976; Pinder et al., 1979; Flanagan & Lin, 1980). Furthermore, gelsolin (Yin et al., 1981b), villin (Craig & Powell, 1980; Glenney et al., 1981), and related proteins [e.g., see Wang & Bryan (1981)] that accelerate actin polymerization are thought to provide stable complexes with actin which act as nuclei, thereby eliminating the slow phase of filament assembly.

The nucleating capacity of plasma ADF is markedly stimulated by calcium ions, with a steep change in k_{obsd} between 10^{-6} and 10^{-7} M (Figure 7). This calcium dependence is similar to that shown by gelsolin for the inhibition of actin

gelation (Yin & Stossel, 1979) and is consistent with the affinity of gelsolin for Ca^{2+} (1.09×10^6 M^{-1}) (Yin & Stossel, 1980). However, in our experiments, Ca^{2+} does not act simply as an "off–on" switch for nucleation, because even at $<10^{-8}$ M calcium, both the rate of polymerization and the extent of polymerization (as determined by the amplitude of the fluorescence changes) are affected by ADF (Figures 8 and 9). At $<10^{-8}$ M calcium, k_{obsd} increases gradually with ADF concentration, while at 10^{-4} M Ca^{2+}, there is a much sharper acceleration of rate, and this becomes independent of ADF concentration at high ratios of ADF to actin (Figure 8). If ADF binds actin monomers to form a nucleating species, then the rate of filament formation will increase with increasing ADF concentration. The slower increase in k_{obsd} at $<10^{-8}$ M calcium may reflect the presence of fewer nuclei due to the weaker binding of the actin monomers required to constitute a nucleus.

When either viscosity or fluorescence is used to follow actin polymerization, there is a progressive decrease in the magnitude of the signal at equilibrium as the concentration of ADF is increased (Figures 3 and 9). This effect is seen whether or not calcium is present, indicating that ADF affects filament formation even at low calcium concentrations. Low molar ratios of ADF to actin produce large changes in equilibrium viscosity; e.g., in Figure 3, 1 ADF:220 actins reduces the viscosity by 35%. This can be explained by the production of shorter filaments, an average of 220 monomers long. Electron microscope studies confirm that polymerization produces progressively shorter filaments with increasing ADF concentration.

A reduction in filament length might not of itself be expected to produce a lower final fluorescence as observed in polymerization experiments in the presence of ADF. However, as discussed by Kirschner (1980), when filaments are capped at their preferred assembly ends, the critical concentration is expected to increase due to the higher dissociation constant at the preferred disassembly ends of the filaments. Experiments by Pollard & Mooseker (1981) to measure the rates of association and dissociation of monomers at both "barbed" and "pointed" ends of actin filaments have confirmed that the dissociation constant at the pointed end is about 3 times greater than that at the barbed end in 4 mM Mg^{2+} and 75 mM KCl at pH 7.0. Our experiments confirm an increase in the critical concentration in the presence of ADF, which is consistent with such a mechanism (Figure 4). The critical concentration was increased from about 0.48 μM in the absence of ADF to about 1.3 μM in 0.02 μM ADF, and in parallel experiments at 0.1 and 0.3 μM ADF, there was a further increase in the critical concentration to 1.5 and 2.0 μM actin, respectively. These results suggest the release of the equivalent of 40 actin monomers per ADF at the lowest ADF concentration used here but only 2–3 monomers per ADF for increments of ADF concentration from 0.02 to 0.1 μM and from 0.1 to 0.3 μM. The substantial initial increase cannot be attributed to ADF–actin complexes but probably reflects the true rise in the critical concentration when the preferred assembly end is blocked. [In a recent publication by Wegner (1982), the critical concentration at the free disassembly end is estimated at >0.5 μM in native actin compared to a net critical concentration of 0.16 μM.] However, the incremental increase calculated above may reflect the presence of ADF–actin complexes (about 1:2 molar ratio) which do not exhibit an F-type fluorescence (see Results). Alternatively, the fluorescence properties of actin monomers at the ends of filaments may resemble the G form: as filaments progressively shorten, the proportion of fluorescence arising from monomers at the ends of filaments will become increasingly significant.

Polymerizations carried out in the presence of calcium and at high ratios of ADF to actin showed an overshoot in which the fluorescence increased rapidly to a maximum and thereafter declined to an equilibrium value. These observations cannot be explained on the basis of a simple nucleation model. Among the possible explanations are (i) that the fluorescence reflects a genuine overshoot in polymerization which is followed by a subsequent slow depolymerization to equilibrium or (ii) that a slower additional process occurs that affects the fluorescence yield. Such a process might include a conformational change, possibly related to the ATP hydrolysis step. [Pardee & Spudich (1982) have shown that ATP hydrolysis can occur subsequent to polymerization.]

ADF addition to *N*-(1-pyrenyl)iodoacetamide-labeled F-actin produced a decline in fluorescence in both the presence and absence of calcium. Thus, complex formation between ADF and actin is Ca^{2+} independent. Interaction of ADF with stabilized actin filaments is very rapid, the fluorescence changes being complete within the mixing time. The fluorescence decreases approximately linearly with ADF concentration (Figure 11A): a 50% loss of fluorescence occurs at an ADF:actin ratio of about 1:5, and extrapolation of the graphs suggests that the titration is complete at an ADF:actin ratio of about 1:2. The simplest interpretation of these results is that the reduction in fluorescence by successive additions of ADF arises either from a lower fluorescence yield of shorter actin filaments or because there is a progressive increase in monomeric actin. We have no evidence to believe that the fluorescence yield of F-actin is length dependent, although as already noted, ends of filaments may influence the fluorescence intensity in the case of very short oligomers. The relationship between the intensity and spectral ratio shown in Figure 11B is that expected for a system containing only G and F forms of fluorescent actin. Intermediates with different spectral properties may exist, but these are neither abundant nor long-lived. However, any intermediates or complexes with spectral properties like G-actin cannot be distinguished from actin monomers. It has been shown previously that at ratios of ADF:actin of >1:20, ADF promotes almost stoichiometric release of the DNase inhibitor from actin filaments (Harris et al., 1982). This inhibitor may be either free monomers or ADF–actin complexes; in either case, these would contribute to a fluorescence decrease.

The mechanism of severing by ADF is not known. Since the fluorescence changes are very rapid and occur with stabilized filaments in the absence of ATP, it seems very unlikely that fragmentation can arise solely by reequilibration of monomers from capped filaments even under conditions where adventitiously sheared filaments are prevented from reannealing. Further experiments to explore the interaction of ADF with fluorescently labeled actin by rapid reaction methods may reveal the presence of other intermediate states in the severing and depolymerization process.

The fluorescence changes on addition of ADF to F-actin in the presence of ATP are much more complex than those in glycerol. At low ratios of ADF:actin (1:500–1:50), the fluorescence intensity falls steadily with increasing ADF concentration, without any noticeable time dependence thereafter. At ratios of 1:50–1:10, the sharp initial fall in fluorescence is followed by a slower decline as shown in Figure 12. Calcium ions have little effect in either of these phases of the reaction. These observations are consistent with filaments being shortened by ADF and an increase in the pro-

portion of G-actin. Critical concentration measurements support this conclusion (Figure 4B). Both viscosity measurements and electron microscopy indicate a reduction in filament length: indeed, electron microscopy suggests that the filament length is roughly that expected from the actin:ADF ratio (Table I).

Comparison of Figures 11 and 12 shows that much less ADF is required to produce a given decrease in the fluorescence intensity when ATP is present, i.e., under conditions where actin may "treadmill". (A 50% drop occurs at about 1 ADF per 20–25 actin monomers.) Under these conditions, capping of filaments would be followed by a loss of monomers from the preferred disassembly ends to raise the critical concentration. At first sight, it could be argued that our results are consistent with this model and that the slow decay in fluorescence corresponds to this monomer loss. However, there is no slow phase in the early stages of the titration (see Figure 12C) where a sequential dissociation of a large number of monomers (>100) from a small number of filament ends would be expected to take several minutes [based on the off rates of Pollard & Mooseker (1981)]. By contrast, filaments containing 10–50 monomers would be expected to produce a similar rise in the critical concentration with a few seconds, yet the half-time observed for the slow fluorescence decay is about 3 min. These observations cannot therefore be explained on the basis of current models for actin filament disassembly, and further experiments are required to distinguish between reactions that influence fluorescence yield and processes involved in the conversion of filamentous to monomeric actin.

The principal conclusion from these studies is that ADF binds to and fragments F-actin in a calcium-insensitive manner, producing shorter filaments, actin monomers, and complexes between ADF and actin. ADF also binds to monomeric actin and nucleates filament assembly. This process is strongly accelerated by Ca^{2+}. One mechanism by which a protein may promote actin nucleation is by binding at least two monomers in the right orientation for assembly. Villin core, a proteolytic fragment of the intestinal microvillus protein villin, which nucleates actin filament assembly, forms a complex with two to three actin monomers in a Ca^{2+}-dependent manner (Glenney et al., 1981). Gelsolin binds 1.6 mol of actin, also in the presence of calcium (Yin et al., 1981b). The calcium-dependent and calcium-independent properties of plasma ADF may be explained at this stage by a hypothetical model in which a single actin monomer is tightly bound in a calcium-insensitive manner but in which Ca^{2+} ions promote the binding of at least one additional monomer per ADF.

Much evidence has accumulated over the past 2 years on the biochemical properties of proteins from a number of sources that regulate actin filament length, notably gelsolin (Yin et al., 1980) and villin (Bretscher & Weber, 1980). From the experiments reported here, the properties of plasma ADF show striking similarities to those of gelsolin, but there are notable differences, particularly in relation to the effects of calcium ions.

Acknowledgments

We thank John Gooch for his tireless efforts in making ADF. We are indebted to Dr. H. E. Huxley for much valued criticism and constructive suggestions on the manuscript. We thank Dr. W. Gratzer, Dr. P. Matsudaira, and B. Pope for helpful discussions.

Registry No. Calcium, 7440-70-2.

References

Bradford, M. M. (1976) *Anal. Biochem. 72*, 248–254.
Bretscher, A., & Weber, K. (1980) *Cell (Cambridge, Mass.) 20*, 839–847.
Chaponnier, C., Borgia, R., Rungger-Brandle, E., Weil, R., & Gabbiani, G. (1979) *Experientia 35*, 1039–1040.
Chibber, B. A. K., Deutsch, D. G., & Mertz, E. T. (1974) *Methods Enzymol. 34*, 424–432.
Cooke, R. (1975) *Biochemistry 14*, 3250–3256.
Craig, R., Szent-Gyorgyi, A. G., Beese, L., Flicker, P., Vibert, P., & Cohen, C. (1980) *J. Mol. Biol. 140*, 35–55.
Craig, S. W., & Powell, L. D. (1980) *Cell (Cambridge, Mass.) 22*, 739–746.
Flanagan, M. D., & Lin, S. (1980) *J. Biol. Chem. 255*, 835–838.
Glenney, J. R., Kaulfus, P., & Weber, K. (1981) *Cell (Cambridge, Mass.) 24*, 471–480.
Gordon, D. J., Yang, Y.-Z., & Korn, E. D. (1976) *J. Biol. Chem. 251*, 7474–7479.
Harafuji, H., & Ogawa, Y. (1980) *J. Biochem. (Tokyo) 87*, 1305–1312.
Harris, D. A., & Schwartz, J. H. (1981) *Proc. Natl. Acad. Sci. U.S.A. 78*, 6798–6802.
Harris, H. E., & Weeds, A. G. (1978) *FEBS Lett. 90*, 84–88.
Harris, H. E., & Gooch, J. G. (1981) *FEBS Lett. 123*, 49–53.
Harris, H. E., Bamburg, J. R., & Weeds, A. G. (1980) *FEBS Lett. 121*, 175–177.
Harris, H. E., Bamburg, J. R., Bernstein, B. W., & Weeds, A. G. (1982) *Anal. Biochem. 119*, 102–114.
Higashi, S., & Oosawa, F. (1965) *J. Mol. Biol. 12*, 843–865.
Huxley, H. E., & Brown, W. (1967) *J. Mol. Biol. 30*, 383–434.
Kasai, M., Asakura, S., & Oosawa, F. (1962) *Biochim. Biophys. Acta 57*, 22–31.
Kawamura, M., & Maruyama, K. (1970) *J. Biochem. (Tokyo) 67*, 437–457.
Kirschner, M. W. (1980) *J. Cell Biol. 86*, 330–334.
Korn, E. D. (1982) *Physiol. Rev. 62*, 672–737.
Kouyama, T., & Mihashi, K. (1981) *Eur. J. Biochem. 114*, 33–38.
Lehrer, S. S., & Kerwar, G. (1972) *Biochemistry 11*, 1211–1216.
Norberg, R., Thorstensson, R., Utter, G., & Fagreus, A. (1979) *Eur. J. Biochem. 100*, 575–583.
Pardee, J. D., & Spudich, J. A. (1982) *J. Cell Biol. 93*, 648–654.
Pinder, J. C., & Gratzer, W. B. (1982) *Biochemistry 21*, 4886–4890.
Pinder, J. C., Ungewickell, E., Calvert, R., Morris, E., & Gratzer, W. B. (1979) *FEBS Lett. 104*, 396–400.
Pollard, T. D., & Mooseker, M. S. (1981) *J. Cell Biol. 88*, 654–659.
Pollard, T. D., & Craig, S. W. (1982) *Trends Biochem. Sci. (Pers. Ed.) 7*, 88–92.
Polson, A., Potgieter, G. M., Largier, J. F., Mears, G. E. F., & Joubert, F. J. (1964) *Biochim. Biophys. Acta 82*, 463–475.
Schliwa, M. (1981) *Cell (Cambridge, Mass.) 25*, 587–590.
Simpson, P. A., & Spudich, J. A. (1980) *Proc. Natl. Acad. Sci. U.S.A. 77*, 4610–4613.
Snabes, M. C., Boyd, A. E., & Bryan, J. (1981) *J. Cell Biol. 90*, 809–812.
Taylor, R. S., & Weeds, A. G. (1976) *Biochem. J. 159*, 301–315.
Tellam, R., & Frieden, C. (1982) *Biochemistry 21*, 3207–3214.
Thorstensson, R., Utter, G., & Norberg, R. (1982) *Eur. J. Biochem. 126*, 11–16.

Wang, L. L., & Bryan, J. (1981) *Cell (Cambridge, Mass.)* *25*, 637–649.
Weeds, A. G. (1982) *Nature (London)* *296*, 811–815.
Wegner, A. (1976) *J. Mol. Biol.* *108*, 139–150.
Wegner, A. (1982) *J. Mol. Biol.* *161*, 607–615.
Wegner, A., & Neuhaus, J.-M. (1981) *J. Mol. Biol.* *153*, 681–693.
Yin, H. L., & Stossel, T. P. (1979) *Nature (London)* *281*, 583–586.
Yin, H. L., & Stossel, T. P. (1980) *J. Biol. Chem.* *255*, 9490–9493.
Yin, H. L., Zaner, K. S., & Stossel, T. P. (1980) *J. Biol. Chem.* *255*, 9494–9500.
Yin, H. L., Albrecht, J. H., & Fattoum, A. (1981a) *J. Cell Biol.* *91*, 901–906.
Yin, H. L., Hartwig, J. H., Maruyama, K., & Stossel, T. P. (1981b) *J. Biol. Chem.* *256*, 9693–9697.
Zechel, K. (1980) *Eur. J. Biochem.* *119*, 209–213.

Immunochemical Studies on the Combining Sites of Forssman Hapten Reactive Hemagglutinins from *Dolichos biflorus*, *Helix pomatia*, and *Wistaria floribunda*†

Donald A. Baker, Shunji Sugii, Elvin A. Kabat,* R. Murray Ratcliffe,‡ Peter Hermentin,§ and Raymond U. Lemieux

ABSTRACT: The lectin of *Dolichos biflorus*, a hemagglutinin previously considered to be blood group A specific, is now found to react much more strongly with the terminal disaccharide unit [αDGalNAc(1→3)βDGalNAc] of the Forssman antigenic determinant. In contrast, the relative reactions of the lectins of *Helix pomatia* (which also agglutinates A erythrocytes) and *Wistaria floribunda* (which agglutinates A, B, and O erythrocytes) with the Forssman pentasaccharide were substantially weaker than that of *Dolichos biflorus*. The combining site of the lectin of *Helix pomatia* has a broader affinity for terminal 2-acetamido-2-deoxy-α-D-galactopyranose (αDGalNAc) residues than does that of *Dolichos biflorus*. The reactions of the lectin with terminal αDGalNAc units are strongly dependent on the nature of the aglycon and remain ill defined. The lectin may also react with appropriately presented terminal 2-acetamido-2-deoxy-β-D-glucopyranose units. The broad affinity of the lectin of *Wistaria floribunda* which reacts both with a range of blood group specific glycoproteins (A, B, H, Le^a, and Le^b) and with non blood group glycoproteins [Sugii, S., & Kabat, E. A. (1980) *Biochemistry* *19*, 1192–1199] appears best assigned to a combining site that favors pauci- or multivalent cooperative effects of clustered terminal β-D-galactopyranose units. An attempt is made to rationalize certain of the inhibition data in terms of topographical features at the surfaces of the carbohydrate structures which are considered compatible for binding within essentially hydrophobic combining sites.

Hemagglutinins (lectins) isolated from various plants and animals have combining sites specific for carbohydrates (Goldstein & Hayes, 1978; Lis & Sharon, 1977; Nicolson, 1974; Pereira & Kabat, 1979). Some lectins induce lymphocyte blast transformation in addition to agglutinating animal red blood cells and malignant cells. These reactions are quite similar to antigen–antibody reactions and are specifically reversible with low molecular weight sugars. Thus, some hemagglutinins with apparently well-defined specificities have been extensively used as tools for detection, characterization, and isolation of materials containing carbohydrate moieties on cell membranes and cell surfaces (Allen & Johnson, 1976; Hudgin et al., 1974; Kawasaki & Ashwell, 1976; Kimura et al., 1979; Nicolson, 1974; Pereira & Kabat, 1976; Poste et al., 1979). Recently, the reactions of 12 lectins with a wide variety of *N*-glycosyl proteins were examined (Debray et al., 1981), and it was concluded "that lectins considered 'identical' in terms of monosaccharide specificity, possess the ability to recognize fine differences in more complex structures". It was also concluded that the results obtained with lectins in reactions with glycoproteins or cell-surface carbohydrates have to be very carefully interpreted.

This paper is concerned with a comparison of the affinities of the *Dolichos biflorus* hemagglutinin with those of *Helix pomatia* and *Wistaria floribunda* since these hemagglutinins all appeared to bind 2-acetamido-2-deoxy-D-galactopyranose (DGalNAc)[1] residues (Cheung et al., 1979; Kurokawa et al.,

† From the Departments of Microbiology, Human Genetics and Development, and Neurology and the Cancer Center/Institute for Cancer Research (S.S. and E.A.K.), Columbia University College of Physicians and Surgeons, New York, New York 10032, and Chembiomed Ltd. (D.A.B. and R.M.R.) and the Department of Chemistry (P.H. and R.U.L.), University of Alberta, Edmonton, Alberta T6G 2G2, Canada. *Received December 14, 1982.* This paper is dedicated to Professor Edgar Lederer on the occasion of his 73rd birthday. Supported by Grant PCM 81-02321 from the National Science Foundation to E.A.K., by Cancer Center Support Grant CA 13696 to Columbia University, and by National Science and Engineering Council of Canada Grant A172 to R.U.L.

* Correspondence should be addressed to this author at the Department of Microbiology, Columbia University College of Physicians and Surgeons.

‡ Professional Research Associate, 1977–1979, University of Alberta.

§ University of Alberta Postdoctoral Fellow, 1979–1981. Present address: Behringwerke AG, Abteilung Mikrobiologie, D-3350 Marburg 1, West Germany.

[1] Abbreviations: DGlc, D-glucopyranose; DGal, D-galactopyranose; LFuc, L-fucopyranose; DMan, D-mannopyranose; Fruc, fructofuranose; LAra, L-arabinose; DManNAc, 2-acetamido-2-deoxy-D-mannopyranose; DGalNAc, 2-acetamido-2-deoxy-D-galactopyranose; DGlcNAc, 2-acetamido-2-deoxy-D-glucopyranose; MeαDGalNAc*p*, methyl 2-acetamido-2-deoxy-α-D-galactopyranoside; MeαDGalNAc*f*, methyl 2-acetamido-2-deoxy-α-D-galactofuranoside; GalNAcol, *N*-acetyl-2-deoxy-D-galactitol; EDTA, ethylenediaminetetraacetic acid; MSS, 10% 2×, fraction of a human ovarian cyst blood group substance precipitated twice from 90% phenol by addition of ethanol to 10% final concentration (MS is the subject, S is serous fluid, and M is mucinous fluid); HSEA, hard sphere exoanomeric molecular orbital calculations (Thøgersen et al., 1982).

0006-2960/83/0422-2741$01.50/0